Frontiers of Physics
https://doi.org/10.1007/s11467-021-1087-4
Front. Phys.
16(5), 51502 (2021)

RESEARCH ARTICLE

Noncyclic nonadiabatic holonomic quantum gates via shortcuts to adiabaticity

Sai Li[1], **Pu Shen**[1], **Tao Chen**[1], **Zheng-Yuan Xue**[1,2,†]

[1] *Guangdong Provincial Key Laboratory of Quantum Engineering and Quantum Materials, and School of Physics and Telecommunication Engineering, South China Normal University, Guangzhou 510006, China*
[2] *Guangdong-Hong Kong Joint Laboratory of Quantum Matter, and Frontier Research Institute for Physics, South China Normal University, Guangzhou 510006, China*
Corresponding author. E-mail: [†] *zyxue83@163.com*
Received March 1, 2021; accepted May 19, 2021

High-fidelity quantum gates are essential for large-scale quantum computation. However, any quantum manipulation will inevitably affected by noises, systematic errors and decoherence effects, which lead to infidelity of a target quantum task. Therefore, implementing high-fidelity, robust and fast quantum gates is highly desired. Here, we propose a fast and robust scheme to construct high-fidelity holonomic quantum gates for universal quantum computation based on resonant interaction of three-level quantum systems via shortcuts to adiabaticity. In our proposal, the target Hamiltonian to induce noncyclic non-Abelian geometric phases can be inversely engineered with less evolution time and demanding experimentally, leading to high-fidelity quantum gates in a simple setup. Besides, our scheme is readily realizable in physical system currently pursued for implementation of quantum computation. Therefore, our proposal represents a promising way towards fault-tolerant geometric quantum computation.

Keywords noncyclic, holonomic quantum gates, shortcuts to adiabaticity, Lewis–Riesenfeld invariant

1 Introduction

Quantum computation, based on the laws of quantum mechanics, is promising in solving hard computational problems and has many potential applications in modern science and technology [1]. However, noises, systematic errors and decoherence effects will inevitably affect a quantum gate operation, which can result in the deviation of the target evolution, i.e., infidelity of a quantum gate. Thus, for large scale quantum computation, noise-resistant and high-fidelity quantum gates are highly desired. Remarkably, geometric phases [2–4] only depend on the global properties of their evolution trajectories, and thus can naturally be used to induce quantum gates that are robust against certain local noises [5–10].

Recently, nonadiabatic holonomic quantum computation (NHQC), based on the non-Abelian geometric phase, has been proposed for high-fidelity quantum operation [11, 12], and then significant theoretical [13–20] and experimental progresses [21–31] have been made. However, the above NHQC implementations are sensitive to the systematic error [32, 33] caused by external control imperfections, which can lead to infidelity of the implemented gate. The main reason for this sensitivity is due to the fact that, in three-level quantum systems, the two coupling strengths in the above implementations need to be synchronized. This strong requirement leads to the fact that the two couplings are actually one independent variable, similar to the case of Rabi oscillation.

In implementing of NHQC, to improve the gate robustness against systematic control errors, various protocols have been proposed with preliminary experimental demonstrations. As the first stage, the conventional encoding methods have been proposed [12, 34–44], which require more resources of physical qubits. Then, other quantum control techniques are introduced in cooperating with NHQC, such as the composite scheme or dynamical decoupling strategy [45–47], the deliberately optimal pulse control technique [48–55], and complex pulses target to shorten the gate-time [56–60]. However, these kinds of enhancement of gate robustness either need deliberate control of experimental pulse or greatly lengthen the gate-time. Therefore, improving the holonomic gate robustness in NHQC with simplified control is highly desired.

Here, to further improve gate robustness in NHQC, we propose a fast and robust scheme to construct high-fidelity holonomic quantum gates based on resonant interaction of three-level quantum systems via shortcuts to adiabaticity (STA) [61, 62]. Specifically, in our scheme, non-synchronous coupling strengths of the Hamiltonian for the target noncyclic holonomic quantum gates can be

* arXiv: 2105.13912. This article can also be found at http://journal.hep.com.cn/fop/EN/10.1007/s11467-021-1087-4.

© Higher Education Press 2021

inversely engineered with the help of the Lewis-Riesenfeld invariant (LRI) [63–68]. Comparing with previous NHQC schemes, our scheme has the following merits. First, we only employ the conventional pulse shaping technique, which is experimentally friendly and can be readily realized in current experiments. Second, arbitrary optimized gate can be achieved with smaller pulse area, which can lead to shorter gate time and thus smaller decoherence-induced gate infidelity. Besides, the gate robustness is greatly enhanced via numerically evaluation. In addition, our scheme can be readily implemented in conventional physical systems for quantum computation, e.g., superconducting quantum circuits, nitrogen-vacancy centres and trapped ions, etc. Therefore, our proposal represents a promising way towards fault-tolerant quantum computation.

2 Hamiltonian engineering via STA

We now introduce how to construct the Hamiltonian for realizing a target evolution based on the LRI theory [63–68]. Here, we consider a Λ-type three-level system that is resonantly driven by two external fields, inducing the coupling between auxiliary state $|e\rangle$ and qubit states $|0\rangle$, $|1\rangle$, respectively, as shown in Fig. 1(a). In addition, our protocol can also be applicable in the V- or Ξ-type configurations. Assuming $\hbar = 1$ hereafter, under the rotating wave approximation, the driven system can be expressed in the subspace $\{|0\rangle, |e\rangle, |1\rangle\}$ as

$$\mathcal{H}(t) = \frac{1}{2}\begin{pmatrix} 0 & \Omega_0(t) & 0 \\ \Omega_0(t) & 0 & \Omega_1(t)\mathrm{e}^{-\mathrm{i}\phi} \\ 0 & \Omega_1(t)\mathrm{e}^{\mathrm{i}\phi} & 0 \end{pmatrix}, \tag{1}$$

where $\Omega_k(t)$ with $k = 0, 1$ represents time-dependent coupling strength between auxiliary state $|e\rangle$ and qubit state $|k\rangle$, and ϕ is a constant relative phase. In general, this time-dependent Hamiltonian $\mathcal{H}(t)$ is difficult to be solved, and thus it is hard to obtain the evolution operator by directly using $U = \hat{\mathcal{T}}\mathrm{e}^{-\mathrm{i}\int_0^T \mathcal{H}(t)\mathrm{d}t}$. Thus, the LRI theory [63–68] has been proposed to find exact solution of the time-dependent Schrödinger equation of $\mathcal{H}(t)$, and thus the corresponding evolution operator can be easily found. In the case of Hamiltonian $\mathcal{H}(t)$, there exists a LRI [67]

$$I(t) = \frac{\lambda}{2}\begin{pmatrix} 0 & \cos\gamma\sin\beta & -\mathrm{i}\sin\gamma\mathrm{e}^{-\mathrm{i}\phi} \\ \cos\gamma\sin\beta & 0 & \cos\gamma\cos\beta\mathrm{e}^{-\mathrm{i}\phi} \\ \mathrm{i}\sin\gamma\mathrm{e}^{\mathrm{i}\phi} & \cos\gamma\cos\beta\mathrm{e}^{\mathrm{i}\phi} & 0 \end{pmatrix}, \tag{2}$$

where λ is a constant, and γ and β are time-dependent variables designed for a target task. Furthermore, by solving $dI/dt \equiv \partial I/\partial t + (1/i)[I(t), \mathcal{H}(t)] = 0$, constraint conditions between the coupling strength $\Omega_k(t)$ and the invariant parameters can be obtained as

$$\begin{aligned} \Omega_0(t) &= 2[\dot{\beta}\cot\gamma(t)\sin\beta(t) + \dot{\gamma}\cos\beta(t)], \\ \Omega_1(t) &= 2[\dot{\beta}\cot\gamma(t)\cos\beta(t) - \dot{\gamma}\sin\beta(t)], \end{aligned} \tag{3}$$

where $\dot{\beta}$ and $\dot{\gamma}$ denote the time derivative of $\beta(t)$ and $\gamma(t)$, respectively.

In addition, eigenstates of $I(t)$ can be chosen as

$$|\varphi_0(t)\rangle = \begin{pmatrix} \cos\gamma(t)\cos\beta(t) \\ -\mathrm{i}\sin\gamma(t) \\ -\cos\gamma(t)\sin\beta(t)\mathrm{e}^{\mathrm{i}\phi} \end{pmatrix}, \tag{4}$$

and

$$|\varphi_\pm(t)\rangle = \frac{1}{\sqrt{2}}\begin{pmatrix} \sin\gamma(t)\cos\beta(t) \pm \mathrm{i}\sin\beta(t) \\ \mathrm{i}\cos\gamma(t) \\ [-\sin\gamma(t)\sin\beta(t) \pm \mathrm{i}\cos\beta(t)]\mathrm{e}^{\mathrm{i}\phi} \end{pmatrix}, \tag{5}$$

as a set of orthogonal dressed states, with the corresponding eigenvalues being 0 and $\pm\lambda/2$, respectively. As an arbitrary evolution state $|\psi(t)\rangle$ under the driven Hamiltonian $\mathcal{H}(t)$ can be expanded as a linear superposition of dressed states as $|\psi(t)\rangle = \sum_{n=0,\pm} C_n\mathrm{e}^{\mathrm{i}\alpha_n}|\varphi_n(t)\rangle$ with C_n being time-independent amplitudes, according to the LRI theory, the corresponding LR phase is $\alpha_n(t) = \int_0^t \langle\varphi_n(t')|[\mathrm{i}(\partial/\partial t') - \mathcal{H}(t')]|\varphi_n(t')\rangle\,\mathrm{d}t'$, which is the global phase accumulated on a dressed state. This LR phase includes both geometric (first term) and dynamical (second term) parts. Then, the time-evolution operator is

$$U(t) = \sum_{n=0,\pm} \mathrm{e}^{\mathrm{i}\alpha_n}|\varphi_n(t)\rangle\langle\varphi_n(0)|, \tag{6}$$

where $\alpha_\pm(t) = \mp\int_0^t \dot{\beta}(t')/\sin\gamma(t')\mathrm{d}t'$ and $\alpha_0 = 0$. That is, according to the required properties of α_n, after properly designing time-dependent variables β, γ and the time-independent ϕ, a target Hamiltonian $\mathcal{H}(t)$ can be inversely engineered according to Eq. (3), and the resulting time-evolution operator of the qubit system is determined by Eq. (6).

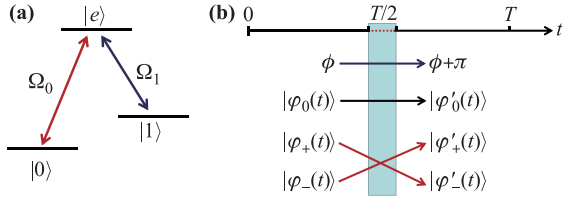


Fig. 1 **(a)** The coupling configuration for a three-level system to induce holonomic quantum gates. **(b)** The schematic show of the construction of the evolution path, where the change of the constant phase factor from ϕ to $\phi + \pi$ of the Hamiltonian in Eq. (1) at $T/2$ leads to the exchange between the two orthogonal channels $|\varphi_\pm(t)\rangle$, which is the key to keep the final state staying within the qubit basis.

3 Holonomic quantum gates

In this section, we present the construction of fast and robust holonomic quantum gates based on the non-belian geometric phase, by applying the strategy of inverse-engineering Hamiltonian described above. Meanwhile, the gate performance is numerically evaluated, which proves that our scheme is more robust than the conventional NHQC scheme [15], under same conditions.

3.1 Gate construction

We first proceed to the holonomic gate construction.A For the purpose of removing dynamical phase and realizing pure non-Abelian geometric evolution, we deliberately divide the evolution path into two equal parts, changing the driving parameters at the intermediate moment as shown in Fig. 1(b). To be specific, in the first part $t \in [0, T/2]$, the boundary conditions are set to be $\phi_1 = \phi$, $\gamma(0) = \gamma(T/2) = 0$, $\beta(0) = \theta/4$ and $\beta(T/2) = 0$. By these settings, according to Eq. (6), the evolution operator of the first part is

$$U(T/2,0) = \sum_{n=0,\pm} \mathrm{e}^{\mathrm{i}\alpha_n(T/2)} |\varphi_n(T/2)\rangle\langle\varphi_n(0)|. \tag{7}$$

Then, in the second part $t \in [T/2, T]$, to make sure that the target states still stay in the qubit subspace and the evolution time is as short as possible, we exchange the two evolution channels $|\varphi_+(t)\rangle$ and $|\varphi_-(t)\rangle$ by changing ϕ to $\phi + \pi$ in the intermediate moment. Besides, we also target to set $\alpha_\pm(T) = -\alpha_\mp(T/2)$ to fully eliminate the dynamical phase. Thus, the boundary conditions can be chosen as $\phi_2 = \phi + \pi$, $\gamma(T/2) = \gamma(T) = 0$, $\beta(T/2) = 0$ and $\beta(T) = \theta/4$, resulting in the evolution operator for the second part as

$$U(T,T/2) = \sum_{n=0,\pm} \mathrm{e}^{\mathrm{i}\alpha_n(T)} |\varphi_n'(T)\rangle\langle\varphi_n'(T/2)|. \tag{8}$$

In this way, during the whole evolution time T, the non-Abelian geometric evolution operator within the quit subspace $\{|0\rangle, |1\rangle\}$ is

$$\begin{aligned} U(T) &= U(T,T/2)U(T/2,0) \\ &= \begin{pmatrix} \cos\frac{\theta}{2} & -\sin\frac{\theta}{2}\mathrm{e}^{-\mathrm{i}\phi} \\ \sin\frac{\theta}{2}\mathrm{e}^{\mathrm{i}\phi} & \cos\frac{\theta}{2} \end{pmatrix}, \end{aligned} \tag{9}$$

which can be regarded as rotation around axis $\cos\phi\sigma_y - \sin\phi\sigma_x$ by an angle $\theta \in [0, \pi]$ denoted as $R[\theta, \phi]$. Thus, by choosing different (θ, ϕ), universal holonomic single-qubit gates can be realized.

3.2 Gate performance

Here, we choose a proper set of time-dependent variables, which satisfy the boundary conditions [66], to show the performance of the implemented holonomic quantum gates. That is, in the first time interval $t \in [0, T/2]$, we set

$$\begin{aligned} \gamma(t) &= -\frac{A}{(T/4)^4} t^2 (t - T/2)^2, \\ \beta(t) &= 35\theta \left[\frac{(T/2-t)^4}{4(T/2)^4} - \frac{3(T/2-t)^5}{5(T/2)^5} \right. \\ &\quad \left. + \frac{(T/2-t)^6}{2(T/2)^6} - \frac{(T/2-t)^7}{7(T/2)^7} \right], \end{aligned} \tag{10}$$

where A is a tunable parameter. And, in the second time interval $t \in [T/2, T]$, we set

$$\begin{aligned} \gamma(t) &= \frac{A}{(T/4)^4} (t - T/2)^2 (t - T)^2, \\ \beta(t) &= 35\theta \left[\frac{(t-T/2)^4}{4(T/2)^4} - \frac{3(t-T/2)^5}{5(T/2)^5} \right. \\ &\quad \left. + \frac{(t-T/2)^6}{2(T/2)^6} - \frac{(t-T/2)^7}{7(T/2)^7} \right]. \end{aligned} \tag{11}$$

The above choice of the boundary conditions can ensure the time-dependent variables to be simple and realizable, and the shapes of parameters $\gamma(t)$ and $\beta(t)$ are shown in Fig. 2(a). Then, the corresponding form of Ω_k in Hamiltonian $\mathcal{H}(t)$ can be reversely engineered according to Eq. (3). Notably, we can find that the pulse area S, defined by $S = \frac{1}{2}\int_0^T \sqrt{\Omega_0^2 + \Omega_1^2}\mathrm{d}t$, of a fixed rotation operation is related to the tunable parameter A directly. Therefore, for a certain rotation angle θ, the minimum pulse area $S_{\min}$ can be obtained by adjusting A, as show in Fig. 2(b) for the gate with $\theta = \pi/2$. Moreover, as shown in Fig. 2(c), we also plot the minimum pulse area $S_{\min}$ with respect to

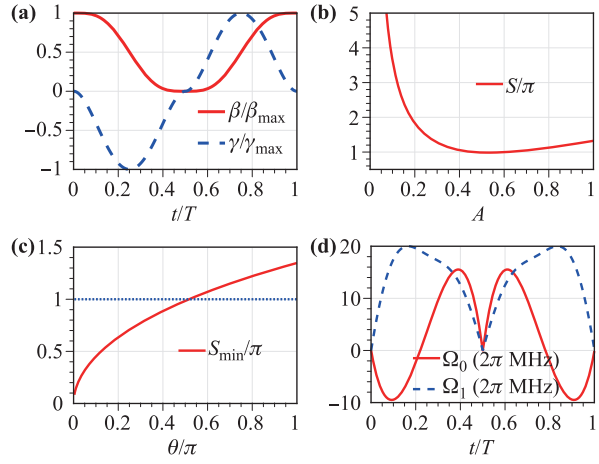


Fig. 2 **(a)** The shapes of the two time-dependent variables of γ and β. **(b)** The pulse area S with respect to A for $\theta = \pi/2$. **(c)** The minimum pulse area S_{min} with respect to θ (red solid line) and the blue dashed line indicates the case of conventional NHQC. **(d)** The slopes of the coupling strength Ω_k for the Hamiltonian in Eq. (1) when $\theta = \pi/2, A = 0.46, T = 29.5$ ns and $S = \pi$.

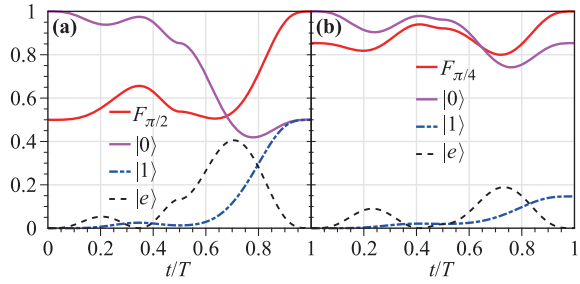


Fig. 3 The dynamics of the state population and fidelity for **(a)** $R[\pi/2,\pi/2]$ and **(b)** $R[\pi/4,\pi/2]$ gate operations.

rotation angle θ. In addition, we can obtain the average gate-time for all possible rotation angle, which indicate that the average gate-time of our scheme is shorter compared with the conventional NHQC case [15] (i.e., $S\equiv\pi$), resulting in higher gate fidelity.

To evaluate the performance of the constructed holonomic gates, we use the Lindblad master equation of

$$\dot{\rho}=\mathrm{i}[\rho,\mathcal{H}(t)]+\frac{1}{2}\left[\Gamma_1\mathcal{L}(\sigma_1)+\Gamma_2\mathcal{L}(\sigma_2)\right], \tag{12}$$

where ρ is the density matrix of the qubit system and $\mathcal{L}(\mathcal{A})=2\mathcal{A}\rho\mathcal{A}^\dagger-\mathcal{A}^\dagger\mathcal{A}\rho-\rho\mathcal{A}^\dagger\mathcal{A}$ is the Lindbladian of operator $\mathcal{A}$; $\sigma_1=|0\rangle\langle e|+|1\rangle\langle e|$ and $\sigma_2=(|e\rangle\langle e|-|0\rangle\langle 0|)+(|e\rangle\langle e|-|1\rangle\langle 1|)$ with Γ_1 and Γ_2 being the corresponding decay and dephasing rates, respectively. Here, considering the energy cost [69, 70] and experimental feasibility, we set the maximum coupling strength to be $(\Omega_k)_{\max}=2\pi\times 20$ MHz. In addition, the decay and dephasing rates are set as $\Gamma_1=\Gamma_2=2\pi\times 5$ kHz. For two typical gate operations $R[\pi/2,\pi/2]$ and $R[\pi/4,\pi/2]$, the minimum pulse area $S_{\min}$ can be obtained with $A=0.46$ and 0.38, respectively. Assuming that the quantum system is initially prepared in $|\psi_1\rangle=|0\rangle$, the obtained gate-fidelities of $R[\pi/2,\pi/2]$ and $R[\pi/4,\pi/2]$ are as high as $F_{\pi/2}=99.91\%$ and $F_{\pi/4}=99.97\%$, as shown in Figs. 3(a) and (b), respectively, where the state fidelity is defined by $F_\theta=\langle\psi_{f_\theta}|\rho|\psi_{f_\theta}\rangle$ with $|\psi_{f_\theta}\rangle=R[\theta,\pi/2]|0\rangle$ being ideal final state. In addition, for a general initial state $|\psi_1\rangle=\cos\theta'|0\rangle+\sin\theta'|1\rangle$, gate operations $R[\pi/2,\pi/2]$ and $R[\pi/4,\pi/2]$ will result in ideal final state $|\psi_{f_\theta}\rangle=\cos\theta'(\cos(\theta/2)|0\rangle+\mathrm{i}\sin(\theta/2)|1\rangle)+\sin\theta'(-\mathrm{i}\sin(\theta/2)|0\rangle+\cos(\theta/2)|1\rangle)$. To fully evaluate the performance of these two gates, the gate-fidelity can be defined as $F_\theta^G=\frac{1}{2\pi}\int_0^{2\pi}\langle\psi_{f_\theta}|\rho_1|\psi_{f_\theta}\rangle\mathrm{d}\theta'$ [71], where the integration is numerically performed for 1001 input states with θ' being uniformly distributed over $[0,2\pi]$, and we obtain the fidelities of the two gates as $F_{\pi/2}^G=99.84\%$ and $F_{\pi/4}^G=99.92\%$, respectively.

3.3 Gate robustness

Different to the conventional NHQC case, the holonomic gates here are implemented with non-synchronous coupling strengths Ω_k. Therefore, we further numerically simulate the gate robustness of these two cases, against

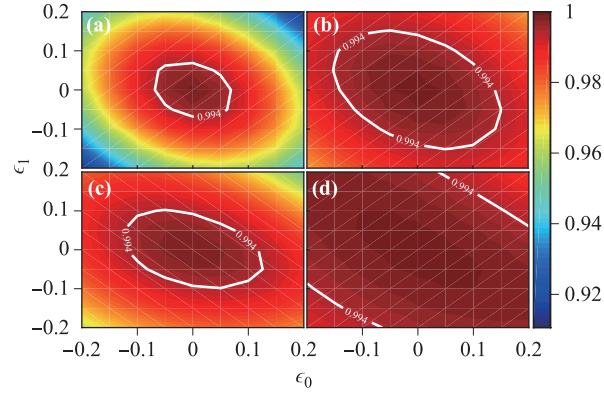


Fig. 4 Gate fidelities under systematic Rabi errors. **(a)** and **(b)** describe the fidelities of the $R_X[\pi/2]$ and $R_X[\pi/4]$ gates in the NHQC case. **(c)** and **(d)** present the fidelities of $R[\pi/2,\pi/2]$ and $R[\pi/4,\pi/2]$ gates in our noncyclic scheme.

the static systematic Rabi errors. Under this error, the interaction Hamiltonian $H(t)$ in Eq. (1) changes to

$$\mathcal{H}'(t)=\frac{1}{2}\begin{pmatrix}0&(1+\epsilon_0)\Omega_0&0\\(1+\epsilon_0)\Omega_0&0&(1+\epsilon_1)\Omega_1\mathrm{e}^{-\mathrm{i}\phi}\\0&(1+\epsilon_1)\Omega_1\mathrm{e}^{\mathrm{i}\phi}&0\end{pmatrix}, \tag{13}$$

where ϵ_k are the static systematic Rabi error fractions. In the following, we use Hamiltonian $\mathcal{H}'(t)$ and the Lindblad master equation in Eq. (12) to evaluate the robustness of the quantum gates for our scheme and the conventional NHQC scheme.

To compare our proposal with the NHQC case under the same conditions, we simulate gate performance in the NHQC case with the same pulse shape of Ω_1, as shown in Fig. 2(d). Furthermore, the evolution operator of our scheme $R[\theta,\pi/2]$ is coincident with $R_X[\theta]$ of the NHQC case, which is a rotating operator around the σ_x axis with an angle θ. As shown in Fig. 4(a) and Fig. 4(b), we simulate the fidelities of $R_X[\pi/2]$ and $R_X[\pi/4]$ gates for the

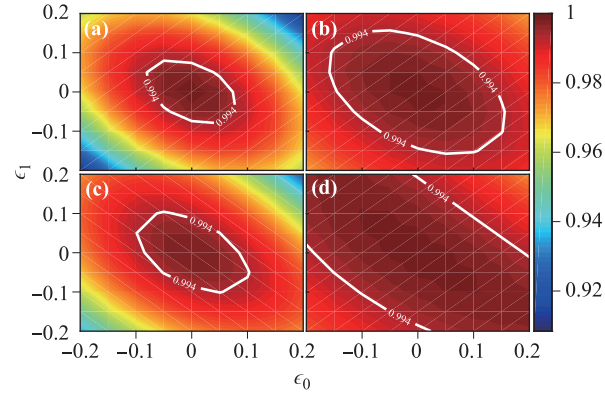


Fig. 5 Gate fidelities under systematic Rabi errors. **(a)** and **(b)** describe the fidelities of the $R_Y[\pi/2]$ and $R_Y[\pi/4]$ gates in the NHQC case. **(c)** and **(d)** present the fidelities of $R[\pi/2,0]$ and $R[\pi/4,0]$ gates in our noncyclic scheme.

NHQC case, with $-0.2 \leq \epsilon_k \leq 0.2$, respectively. And the fidelities of $R[\pi/2, \pi/2]$ and $R[\pi/4, \pi/2]$ gates in our scheme are shown in Fig. 4(c) and Fig. 4(d). It clearly indicates that our scheme is more robust than the NHQC case. Besides, $R[\theta, 0]$ corresponds to $R_Y[\theta]$, which is the rotation around the σ_y axis. And the numerical simulation results of the $R_Y[\pi/2]$ and $R_Y[\pi/4]$ gate-fidelities are shown in Figs. 5(a) and (b), respectively. For comparison purpose, as shown in Figs. 5(c) and (d), gate-fidelities of the evolution operator $R[\pi/2, 0]$ and $R[\pi/4, 0]$ are numerically evaluated, respectively. The simulation result also indicates that our scheme is more robust than the NHQC case. Notably, in the above simulations, we have set the pulse areas of all gates to be $S = \pi$, which is the best performance of NHQC but not ours. That is, S_{min} in our scheme can be smaller than π, i.e., our gate can be faster than the NHQC case and the gate-fidelities present here is not the best ones for our scheme. Therefore, our scheme can implement high-fidelity, robust and low area quantum gates.

4 Physical implementation

In this section, we present the implementation of our proposal on superconducting circuits and nitrogen-vacancy centres, which is directly realizable with current technology. On superconducting circuits, we consider the transmon device, a kind of well-known artificial atom, which possesses a series of nonequal energy levels. Here, our implementation involves the three lowest levels $|g\rangle$, $|e\rangle$ and $|f\rangle$, with $|g\rangle$ and $|f\rangle$ being the qubit-states and $|e\rangle$ is an auxiliary state [21, 28]. Then, two microwave fields $\Omega_l(t)\cos(\omega_l t + \phi_l)$ $(l = 1, 2)$ are resonantly coupled to sequential transitions of these three lowest levels, where $\Omega_l(t)$, ω_l and ϕ_l are time-dependent driving amplitudes, time-independent driving frequencies and phases, respectively. Setting the energy of $|g\rangle$ as the zero point, the original Hamiltonian of the system can be written as

$$\mathcal{H}_1 = \omega_e|e\rangle\langle e| + \omega_f|f\rangle\langle f| + \sum_l \Omega_l(t)\cos(\omega_l t + \phi_l)(b + b^\dagger), \tag{14}$$

where $b = |g\rangle\langle e| + \sqrt{2}|e\rangle\langle f|$ being the annihilation operator of the transmon. In this setting, in the interaction picture and under the rotating wave approximation, the Hamiltonian $\mathcal{H}(t)$ in Eq. (1) of our proposal can be obtained. Moreover, the decay and dephasing rates of a transmon are both on the kHz level [72], as used in our numerics.

In addition, a Hamiltonian for holonomic two-qubit gates is also realizable with auxiliary qubit or cavity coupled two qubits [16, 38, 40, 51]. Specifically, we consider two transmon qubits with frequencies ω_{ge}^k $(k = 0, 1)$ dispersively coupled to an auxiliary transmon with frequency ω_{ge}^A with the detuning being $\Delta_k = \omega_{ge}^k - \omega_{ge}^A$. Meanwhile, two qubits are respectively driven by two microwave fields $\Omega_k(t)\cos(\omega_k(t)t + \phi_k)$ with $\omega_{ge}^k + \omega_{ef}^k - \omega_{ge}^A \approx \omega_k(0)$, where $\omega_k(t)$ is time-dependently adjusted to compensate the interaction-induced ac Stark-shifts of the transmons. In the rotating framework with respect to the driving frequency, the Hamiltonian of the kth qubit coupled to the auxiliary transmon can be written as

$$\begin{aligned}\mathcal{H}_0 &= \delta_k N_k - \frac{\alpha_k}{2}(N_k - 1)N_k + \delta_A N_A - \frac{\alpha_A}{2}(N_A - 1)N_A,\\ \mathcal{H}_I &= g_k a b_k^\dagger + \frac{\Omega_k(t)e^{i\phi_k}}{2} b_k + \text{H.c.},\end{aligned} \tag{15}$$

where $\mathcal{H}_0$ is free Hamiltonian of the coupled system, and the first two terms are nonlinear energy levels of kth transmon with its anharmonicity being α_k, and last two terms are nonlinear energy levels of the auxiliary transmon with the anharmonicity being α_A, and $\delta_k = \omega_{ge}^k - \omega_k$, $\delta_A = \omega_{ge}^A - \omega_k$, $N_k = b_k^\dagger b_k$, $N_A = a^\dagger a$, with b_k and a being the annihilation operator of the qubit and auxiliary transmons, respectively. $\mathcal{H}_I$ is the linear coupling term including the coupling between two transmons with strength g_k and the driven induced interaction on qubit k with strength Ω_k. Then, in the single-excitation subspace $\mathcal{S}_1 = \text{span}\{|fgg\rangle, |ggf\rangle, |geg\rangle\}$, where $|ijk\rangle \equiv |i\rangle \otimes |j\rangle \otimes |k\rangle$ labels product states of two qubits and auxiliary transmon, the effective Hamiltonian can be described as

$$\mathcal{H}_{\text{eff}} = \tilde{g}_1 e^{-i\phi_1}|fgg\rangle\langle geg| + \tilde{g}_2 e^{-i\phi_2}|ggf\rangle\langle geg| + \text{H.c.}, \tag{16}$$

where $\tilde{g}_k = g_k\Omega_k(t)\alpha_k/[\sqrt{2}\Delta_k(\Delta_k - \alpha_k)]$. Thus, the Hamiltonian $\mathcal{H}(t)$ in Eq. (1) of our proposal can be achieved in this two-qubit subspaces, and thus holonomic two-qubit gates can also be obtained, similar to the single-qubit case.

For a nitrogen-vacancy centre in a diamond [23], there is a spin-triplet ground state. The Zeeman components $|m = 0, \pm 1\rangle$ induced by a magnetic field can be defined as $|m = -1\rangle \equiv |0\rangle$ and $|m = 1\rangle \equiv |1\rangle$ as the qubit basis and $|m = 0\rangle \equiv |a\rangle$ as an ancillary state. The transitions from the qubit basis $|0\rangle$ and $|1\rangle$ to the ancillary state $|a\rangle$ are respectively induced by two resonant microwave pulses $\Omega_j(t)\cos(\omega_j t + \phi_j)$ $(j = 1, 2)$, generated by the arbitrary waveform generator. Similar to the above transmon device case, in the interaction picture and within the rotating wave approximation, the Hamiltonian $\mathcal{H}(t)$ in Eq. (1) can also be implemented.

Meanwhile, two-qubits gates for electron and nuclear spins can also be induced with an effective three-level configuration in their coupled system [23]. In this case, a nearby nuclear spin serves as the control qubit with basis vectors being $|\uparrow\rangle$ and $|\downarrow\rangle$. By applying state-selective microwave pulses $\Omega_i(t)\cos(\omega_i t + \phi_i)$ $(i = 1, 2)$ for nuclear spin state $|\uparrow\rangle$, in the interaction picture, the coupling Hamiltonian is

$$\mathcal{H}_2 = \frac{\Omega_1(t)}{2} e^{-i\phi_1}|0\uparrow\rangle\langle a\uparrow|$$

$$+\frac{\Omega_2(t)}{2}\mathrm{e}^{-\mathrm{i}\phi_2}|1\uparrow\rangle\langle a\uparrow|+\mathrm{H.c.}, \quad (17)$$

where $|ij\rangle \equiv |i\rangle \otimes |j\rangle$ labels the product state of the electron and nuclear spins. Thus, the Hamiltonian $\mathcal{H}(t)$ in Eq. (1) can be achieved within this two-qubit subspace, and then holonomic two-qubit gates can be implemented.

5 Conclusion

In conclusion, we have proposed a fast and robust scheme to construct high-fidelity quantum gates for holonomic quantum computation based on resonant interaction of three-level quantum system via STA. In our scheme, combining the transitionless quantum driving with the LRI theory, we have inversely engineered the Hamiltonian with non-synchronous couplings for noncyclic holonomic quantum gates. Meanwhile, by choosing a special evolution path under proper boundary conditions, high-fidelity, robust and low area universal single-qubit gates can be constructed. Furthermore, as verified by numerical simulations, the implemented gates have very high fidelity, and their robustness is stronger than the NHQC case, under the same conditions. Moreover, our scheme can be readily implemented in physical systems, e.g., superconducting circuits and nitrogen-vacancy centres. Therefore, our proposal represents a promising way towards fault-tolerant quantum computation.

Acknowledgements This work was supported by the Key R&D Program of Guangdong Province (Grant No. 2018B030326001), the National Natural Science Foundation of China (Grant No. 11874156), and Science and Technology Program of Guangzhou (Grant No. 2019050001).

References

1. R. P. Feynman, Simulating physics with computers, *Int. J. Theor. Phys.* 21(6–7), 467 (1982)
2. M. V. Berry, Quantal phase factors accompanying adiabatic changes, *Proc. R. Soc. Lond. Ser. A* 392, 45 (1984)
3. F. Wilczek and A. Zee, Appearance of gauge structure in simple dynamical systems, *Phys. Rev. Lett.* 52(24), 2111 (1984)
4. Y. Aharonov and J. Anandan, Phase change during a cyclic quantum evolution, *Phys. Rev. Lett.* 58(16), 1593 (1987)
5. P. Solinas, P. Zanardi, and N. Zanghì, Robustness of non-Abelian holonomic quantum gates against parametric noise, *Phys. Rev. A* 70(4), 042316 (2004)
6. S. L. Zhu, Z. D. Wang, and P. Zanardi, Geometric quantum computation and multiqubit entanglement with superconducting qubits inside a cavity, *Phys. Rev. Lett.* 94(10), 100502 (2005)
7. C. Lupo, P. Aniello, M. Napolitano, and G. Florio, Robustness against parametric noise of nonideal holonomic gates, *Phys. Rev. A* 76(1), 012309 (2007)
8. S. Filipp, J. Klepp, Y. Hasegawa, C. Plonka-Spehr, U. Schmidt, P. Geltenbort, and H. Rauch, Experimental demonstration of the stability of Berry's phase for a spin-1/2 particle, *Phys. Rev. Lett.* 102(3), 030404 (2009)
9. J. Xu, S. Li, T. Chen, and Z. Y. Xue, Nonadiabatic geometric quantum computation with optimal control on superconducting circuits, *Front. Phys.* 15(4), 41503 (2020)
10. Y. Xu, Z. Hua, T. Chen, X. Pan, X. Li, J. Han, W. Cai, Y. Ma, H. Wang, Y. Song, Z. Y. Xue, and L. Sun, Experimental implementation of universal nonadiabatic geometric quantum gates in a superconducting circuit, *Phys. Rev. Lett.* 124(23), 230503 (2020)
11. E. Sjöqvist, D. M. Tong, L. Mauritz Andersson, B. Hessmo, M. Johansson, and K. Singh, Non-adiabatic holonomic quantum computation, *New J. Phys.* 14(10), 103035 (2012)
12. G. F. Xu, J. Zhang, D. M. Tong, E. Sjöqvist, and L. C. Kwek, Nonadiabatic holonomic quantum computation in decoherence-free subspaces, *Phys. Rev. Lett.* 109(17), 170501 (2012)
13. Y. C. Zheng and T. A. Brun, Fault-tolerant holonomic quantum computation in surface codes, *Phys. Rev. A* 91(2), 022302 (2015)
14. G. F. Xu, C. L. Liu, P. Z. Zhao, and D. M. Tong, Nonadiabatic holonomic gates realized by a single-shot implementation, *Phys. Rev. A* 92(5), 052302 (2015)
15. E. Herterich and E. Sjöqvist, Single-loop multiple-pulse nonadiabatic holonomic quantum gates, *Phys. Rev. A* 94(5), 052310 (2016)
16. Z. P. Hong, B. J. Liu, J. Q. Cai, X. D. Zhang, Y. Hu, Z. D. Wang, and Z. Y. Xue, Implementing universal nonadiabatic holonomic quantum gates with transmons, *Phys. Rev. A* 97(2), 022332 (2018)
17. J. Zhang, S. J. Devitt, J. Q. You, and F. Nori, Holonomic surface codes for fault-tolerant quantum computation, *Phys. Rev. A* 97(2), 022335 (2018)
18. T. Chen, J. Zhang, and Z. Y. Xue, Nonadiabatic holonomic quantum computation on coupled transmons with ancillaries, *Phys. Rev. A* 98(5), 052314 (2018)
19. N. Ramberg and E. Sjöqvist, Environment-assisted holonomic quantum maps, *Phys. Rev. Lett.* 122(14), 140501 (2019)
20. C. Wu, Y. Wang, X. L. Feng, and J. L. Chen, Holonomic quantum computation in surface codes, *Phys. Rev. Appl.* 13(1), 014055 (2020)
21. A. A. Jr Abdumalikov, J. M. Fink, K. Juliusson, M. Pechal, S. Berger, A. Wallraff, and S. Filipp, Experimental realization of non-Abelian non-adiabatic geometric gates, *Nature* 496(7446), 482 (2013)
22. G. Feng, G. Xu, and G. Long, Experimental realization of nonadiabatic holonomic quantum computation, *Phys. Rev. Lett.* 110(19), 190501 (2013)
23. C. Zu, W. B. Wang, L. He, W. G. Zhang, C. Y. Dai, F. Wang, and L. M. Duan, Experimental realization of universal geometric quantum gates with solid-state spins, *Nature* 514(7520), 72 (2014)

24. S. Arroyo-Camejo, A. Lazariev, S. W. Hell, and G. Balasubramanian, Room temperature high-fidelity holonomic single-qubit gate on a solid-state spin, *Nat. Commun.* 5(1), 4870 (2014)
25. Y. Sekiguchi, N. Niikura, R. Kuroiwa, H. Kano, and H. Kosaka, Optical holonomic single quantum gates with a geometric spin under a zero field, *Nat. Photonics* 11(5), 309 (2017)
26. B. B. Zhou, P. C. Jerger, V. O. Shkolnikov, F. J. Heremans, G. Burkard, and D. D. Awschalom, Holonomic quantum control by coherent optical excitation in diamond, *Phys. Rev. Lett.* 119(14), 140503 (2017)
27. H. Li, Y. Liu, and G. L. Long, Experimental realization of single-shot nonadiabatic holonomic gates in nuclear spins, *Sci. China Phys. Mech. Astron.* 60(8), 080311 (2017)
28. Y. Xu, W. Cai, Y. Ma, X. Mu, L. Hu, T. Chen, H. Wang, Y. P. Song, Z. Y. Xue, Z. Q. Yin, and L. Sun, Single-loop realization of arbitrary nonadiabatic holonomic single-qubit quantum gates in a superconducting circuit, *Phys. Rev. Lett.* 121(11), 110501 (2018)
29. N. Ishida, T. Nakamura, T. Tanaka, S. Mishima, H. Kano, R. Kuroiwa, Y. Sekiguchi, and H. Kosaka, Universal holonomic single quantum gates over a geometric spin with phase-modulated polarized light, *Opt. Lett.* 43(10), 2380 (2018)
30. K. Nagata, K. Kuramitani, Y. Sekiguchi, and H. Kosaka, Universal holonomic quantum gates over geometric spin qubits with polarised microwaves, *Nat. Commun.* 9(1), 3227 (2018)
31. D. J. Egger, M. Ganzhorn, G. Salis, A. Fuhrer, P. Muller, P. K. Barkoutsos, N. Moll, I. Tavernelli, and S. Filipp, Entanglement generation in superconducting qubits using holonomic operations, *Phys. Rev. Appl.* 11(1), 014017 (2019)
32. S. B. Zheng, C. P. Yang, and F. Nori, Comparison of the sensitivity to systematic errors between nonadiabatic non-Abelian geometric gates and their dynamical counterparts, *Phys. Rev. A* 93(3), 032313 (2016)
33. J. Jing, C. H. Lam, and L. A. Wu, Non-Abelian holonomic transformation in the presence of classical noise, *Phys. Rev. A* 95(1), 012334 (2017)
34. Y. C. Zheng and T. A. Brun, Fault-tolerant scheme of holonomic quantum computation on stabilizer codes with robustness to low-weight thermal noise, *Phys. Rev. A* 89(3), 032317 (2014)
35. J. Zhang, L. C. Kwek, E. Sjöqvist, D. M. Tong, and P. Zanardi, Quantum computation in noiseless subsystems with fast non-Abelian holonomies, *Phys. Rev. A* 89(4), 042302 (2014)
36. Z. T. Liang, Y. X. Du, W. Huang, Z. Y. Xue, and H. Yan, Nonadiabatic holonomic quantum computation in decoherence-free subspaces with trapped ions, *Phys. Rev. A* 89(6), 062312 (2014)
37. J. Zhou, W. C. Yu, Y. M. Gao, and Z. Y. Xue, Cavity QED implementation of non-adiabatic holonomies for universal quantum gates in decoherence-free subspaces with nitrogen-vacancy centers, *Opt. Express* 23(11), 14027 (2015)
38. Z. Y. Xue, J. Zhou, and Z. D. Wang, Universal holonomic quantum gates in decoherence-free subspace on superconducting circuits, *Phys. Rev. A* 92(2), 022320 (2015)
39. Y. Wang, J. Zhang, C. Wu, J. Q. You, and G. Romero, Holonomic quantum computation in the ultrastrong-coupling regime of circuit QED, *Phys. Rev. A* 94(1), 012328 (2016)
40. Z. Y. Xue, J. Zhou, Y. M. Chu, and Y. Hu, Nonadiabatic holonomic quantum computation with all-resonant control, *Phys. Rev. A* 94(2), 022331 (2016)
41. Z. Y. Xue, F. L. Gu, Z. P. Hong, Z. H. Yang, D. W. Zhang, Y. Hu, and J. Q. You, Nonadiabatic holonomic quantum computation with dressed-state qubits, *Phys. Rev. Appl.* 7(5), 054022 (2017)
42. P. Z. Zhao, G. F. Xu, Q. M. Ding, E. Sjöqvist, and D. M. Tong, Single-shot realization of nonadiabatic holonomic quantum gates in decoherence-free subspaces, *Phys. Rev. A* 95(6), 062310 (2017)
43. L. N. Ji, T. Chen, and Z. Y. Xue, Scalable nonadiabatic holonomic quantum computation on a superconducting qubit lattice, *Phys. Rev. A* 100(6), 062312 (2019)
44. Y. Wang, Y. Su, X. Chen, and C. Wu, Dephasing-protected scalable holonomic quantum computation on a Rabi lattice, *Phys. Rev. Appl.* 14(4), 044043 (2020)
45. G. F. Xu, P. Z. Zhao, T. H. Xing, E. Sjöqvist, and D. M. Tong, Composite nonadiabatic holonomic quantum computation, *Phys. Rev. A* 95(3), 032311 (2017)
46. Z. Zhu, T. Chen, X. Yang, J. Bian, Z. Y. Xue, and X. Peng, Single-loop and composite-loop realization of nonadiabatic holonomic quantum gates in a decoherence-free subspace, *Phys. Rev. Appl.* 12(2), 024024 (2019)
47. Y. Sekiguchi, Y. Komura, and H. Kosaka, Dynamical decoupling of a geometric qubit, *Phys. Rev. Appl.* 12(5), 051001 (2019)
48. B. J. Liu, Z. H. Huang, Z. Y. Xue, and X. D. Zhang, Superadiabatic holonomic quantum computation in cavity QED, *Phys. Rev. A* 95(6), 062308 (2017)
49. B. J. Liu, X. K. Song, Z. Y. Xue, X. Wang, and M. H. Yung, Plug-and-play approach to nonadiabatic geometric quantum gates, *Phys. Rev. Lett.* 123(10), 100501 (2019)
50. T. Yan, B. J. Liu, K. Xu, C. Song, S. Liu, Z. Zhang, H. Deng, Z. Yan, H. Rong, K. Huang, M. H. Yung, Y. Chen, and D. Yu, Experimental realization of nonadiabatic shortcut to non-Abelian geometric gates, *Phys. Rev. Lett.* 122(8), 080501 (2019)
51. S. Li, T. Chen, and Z. Y. Xue, Fast holonomic quantum computation on superconducting circuits with optimal control, *Adv. Quantum Technol.* 3(3), 2000001 (2020)
52. M. Z. Ai, S. Li, Z. Hou, Z. Y. Xue, J. M. Cui, Y. F. Huang, C. F. Li, and G. C. Guo, Experimental realization of nonadiabatic holonomic single-qubit quantum gates with optimal control in a trapped ion, *Phys. Rev. Appl.* 14(5), 054062 (2020)
53. M. Z. Ai, S. Li, Z. Y. Xue, J. M. Cui, Y. F. Huang, C. F. Li, and G. C. Guo, Experimental realization of nonadiabatic holonomic single-qubit quantum gates with two dark paths in a trapped ion, arXiv: 2101.07483 (2021)

54. B. J. Liu, Y. S. Wang, and M. H. Yung, Global property condition-based non-adiabatic geometric quantum control, arXiv: 2008.02176 (2020)
55. S. Li and Z. Y. Xue, Dynamically corrected nonadiabatic holonomic quantum gates, arXiv: 2012.09034 (2020)
56. G. F. Xu, D. M. Tong, and E. Sjöqvist, Path-shortening realizations of nonadiabatic holonomic gates, *Phys. Rev. A* 98(5), 052315 (2018)
57. F. Zhang, J. Zhang, P. Gao, and G. Long, Searching nonadiabatic holonomic quantum gates via an optimization algorithm, *Phys. Rev. A* 100(1), 012329 (2019)
58. T. Chen, P. Shen, and Z. Y. Xue, Robust and fast holonomic quantum gates with encoding on superconducting circuits, *Phys. Rev. Appl.* 14(3), 034038 (2020)
59. B. J. Liu, Z. Y. Xue, and M. H. Yung, Brachistochrone non-Adiabatic holonomic quantum control, arXiv: 2001.05182 (2020)
60. Z. Han, Y. Dong, B. Liu, X. Yang, S. Song, L. Qiu, D. Li, J. Chu, W. Zheng, J. Xu, T. Huang, Z. Wang, X. Yu, X. Tan, D. Lan, M. H. Yung, and Y. Yu, Experimental realization of universal time-optimal non-Abelian geometric gates, arXiv: 2004.10364 (2020)
61. X. Chen, A. Ruschhaupt, S. Schmidt, A. del Campo, D. Gu'ery-Odelin, and J. G. Muga, Fast optimal frictionless atom cooling in harmonic traps: Shortcut to adiabaticity, *Phys. Rev. Lett.* 104(6), 063002 (2010)
62. D. Guéry-Odelin, A. Ruschhaupt, A. Kiely, E. Torrontegui, S. Martínez-Garaot, and J. G. Muga, Shortcuts to adiabaticity: Concepts, methods, and applications, *Rev. Mod. Phys.* 91(4), 045001 (2019)
63. H. R. Jr Lewis and W. B. Riesenfeld, An exact quantum theory of the time-dependent harmonic oscillator and of a charged particle in a time-dependent electromagnetic field, *J. Math. Phys.* 10(8), 1458 (1969)
64. X. Chen and J. G. Muga, Engineering of fast population transfer in three-level systems, *Phys. Rev. A* 86(3), 033405 (2012)
65. Y. H. Chen, Z. C. Shi, J. Song, and Y. Xia, Invariant-based inverse engineering for fluctuation transfer between membranes in an optomechanical cavity system, *Phys. Rev. A* 97(2), 023841 (2018)
66. J. Zhou, S. Li, T. Chen, and Z. Y. Xue, Fast hybrid quantum state transfer and entanglement generation via no transition passage, *Ann. Phys. (Berlin)* 531(4), 1800402 (2019)
67. Y. Yan, Y. Li, A. Kinos, A. Walther, C. Y. Shi, L. Rippe, J. Moser, S. Kröll, and X. Chen, Inverse engineering of shortcut pulses for high fidelity initialization on qubits closely spaced in frequency, *Opt. Express* 27(6), 8267 (2019)
68. T. Chen and Z. Y. Xue, High-fidelity and robust geometric quantum gates that outperform dynamical ones, *Phys. Rev. Appl.* 14(6), 064009 (2020)
69. Y. Zheng, S. Campbell, G. De Chiara, and D. Poletti, Cost of counterdiabatic driving and work output, *Phys. Rev. A* 94(4), 042132 (2016)
70. O. Abah, R. Puebla, A. Kiely, G. De Chiara, M. Paternostro, and S. Campbell, Energetic cost of quantum control protocols, *New J. Phys.* 21(10), 103048 (2019)
71. J. F. Poyatos, J. I. Cirac, and P. Zoller, Complete characterization of a quantum process: The two-bit quantum gate, *Phys. Rev. Lett.* 78(2), 390 (1997)
72. M. J. Peterer, S. J. Bader, X. Jin, F. Yan, A. Kamal, T. J. Gudmundsen, P. J. Leek, T. P. Orlando, W. D. Oliver, and S. Gustavsson, Coherence and decay of higher energy levels of a superconducting transmon qubit, *Phys. Rev. Lett.* 114(1), 010501 (2015)